Published paper

Full-scale shaking table tests on a substandard RC building repaired and strengthened with Post-Tensioned Metal Straps

(Short Version: Shake table tests on PTMS-strengthened RC frames)

Reyes Garcia[*1a], Iman Hajirasouliha[1b], Maurizio Guadagnini[1c], Yasser Helal[1d], Yaser Jemaa[1d], Kypros Pilakoutas[1e], Philippe Mongabure [2f], Christis Chrysostomou[3g], Nicholas Kyriakides[3h], Alper Ilki[4i], Mihai Budescu[5j], Nicolae Taranu[5k], Mihaela Anca Ciupala[6l], Lluis Torres[7m], M. Saiidi[8n]

[1]The University of Sheffield, Sheffield, UK; [2]CEA DEN/DANS/DM2S/SEMT/EMSI, Saclay, France; [3]Cyprus University of Technology, Limassol, Cyprus; [4]Istanbul Technical University, Istanbul, Turkey; [5]Technical University "Gheorghe Asachi", Iasi, Romania; [6]University of East London, London, UK; [7]University of Girona, Girona, Spain; [8]University of Nevada, Reno, USA.

Abstract

The effectiveness of a novel Post-Tensioned Metal Strapping (PTMS) technique at enhancing the seismic behaviour of a substandard RC building was investigated through full-scale shake-table tests during the EU-funded project BANDIT. The building had inadequate reinforcement detailing in columns and joints to replicate old construction practices. After the bare building was initially damaged significantly, it was repaired and strengthened with PTMS to perform additional seismic tests. The PTMS technique improved considerably the seismic performance of the tested building. Whilst the bare building experienced critical damage at an earthquake of PGA=0.15g, the PTMS-strengthened building sustained a PGA=0.35g earthquake without compromising stability.

Keywords: shaking table tests, seismic strengthening, substandard RC buildings, beam-column joints Post-Tensioned Metal Straps, inter-storey drift

[*a] Corresponding author, BANDIT Project Engineer Coordinator, email: r.garcia@sheffield.ac.uk, T. +44 114 2225071
[b] Lecturer, i.hajirasouliha@sheffield.ac.uk
[c] Lecturer, m.guadagnini@sheffield.ac.uk
[d] Graduate students, y.helal@sheffield.ac.uk & y.jemaa@sheffield.ac.uk
[e] Professor, BANDIT Group Leader, k.pilakoutas@sheffield.ac.uk
[f] BANDIT Test Engineer, philippe.mongabure@cea.fr
[g] Associate Professor, c.chrysostomou@cut.ac.cy
[h] Post-Doctoral Researcher, n_kyriakides@cytanet.com.cy
[i] Professor, ailki@itu.edu.tr
[j] Professor, mbudescu@ce.tuiasi.ro
[k] Professor taranu@tuiasi.ro
[l] Senior Lecturer, m.a.ciupala@uel.ac.uk
[m] Professor, lluis.torres@udg.edu
[n] Professor, saiidi@unr.edu

1 Introduction

Recent severe earthquakes in developing countries (Kashmir, 2005; China, 2008; Indonesia, 2009; Haiti, 2010) caused numerous casualties and financial losses due to the collapse of many reinforced concrete (RC) buildings. Many structural failures were attributed to the inadequate behaviour of beam-column joints. Typical deficiencies in joints may include [Beres et al., 1996]:

1. Lack of internal steel stirrups (confinement) in the joint core

2. Short anchorage length of bottom beam reinforcement in joint core, and

3. Construction joints above and/or below beam-column joints

Therefore, the local strengthening of substandard joints is essential to reduce the seismic vulnerability of such deficient buildings.

Different techniques have been used for the repair and strengthening of substandard exterior RC beam-column joints, including:

- Crack injection and/or epoxy mortar repair [e.g. Karayannis et al., 1998]

- Concrete/shotcrete jacketing [e.g. Corazao and Durrani, 1989; Karayannis et al., 2008; Tsonos, 2008; 2010]

- Steel jacketing or steel plates [e.g. Corazao and Durrani, 1989; Ghobarah et al., 1996; Biddah et al., 1997; Sasmal et al., 2011]

- Externally bonded fibre reinforced polymers (FRP) [e.g. Gergely et al., 2000; Granata and Parvin, 2001; Ghobarah and Said, 2001; 2002; Antonopoulos and Triantafillou, 2003; Said and Nehdi, 2004; Ghobarah and El-Amoury, 2005; Pantelides and Gergely, 2008; Karayannis and Sirkelis, 2008; Tsonos, 2008; Akguzel and Pampanin, 2010; Alsayed et al., 2010; Le-Trung et al., 2010; Parvin et al., 2010; Al-Salloum et al., 2011; Ilki et al., 2011; Sezen, 2012].

These strengthening techniques were proven very effective at enhancing the ductility and capacity of beam-column joint specimens, as well as the global behaviour of full-scale buildings [e.g. Pinto et al., 2002; Balsamo et al., 2005a; 2005b; Della Corte et al., 2006; Di Ludovico et al., 2008; Garcia et al.,

2010]. However, despite the extensive amount of research studies on strengthening techniques for deficient RC structures, it is important to develop simple and low-cost post-earthquake strengthening solutions for substandard structures, especially for developing countries.

Early work by Frangou et al. [1995; 1996] led to the development of a novel strengthening technique for RC beams and columns using Post-Tensioned Metal Strapping (PTMS). The PTMS technique involves the post-tensioning of high-strength steel straps (bands) around RC members using hydraulically-operated steel strapping tools similar to those utilised in the packaging industry (see Fig. 1). After post-tensioning, the straps are fastened mechanically using "push type" seals to maintain the tensioning force. This provides active confinement to members, thus increasing their ductility and capacity. In comparison to other strengthening techniques, PTMS has advantages such as ease and speed of application, low material cost, ease of removing/replacing damaged straps, and flexibility to strengthen different types of structural elements. The cost and speed of PTMS strengthening technique depend on different factors such as material and labour costs and skill of technical staff. The use of PTMS in developing countries is expected to lead to more cost-effective solutions compared to strengthening methods such as externally bonded FRP reinforcement.

Moghaddam et al. [2010a] carried out tests on 72 small-scale circular and square concrete columns confined with PTMS using different volumetric confinement ratios (i.e. different strap spacing and one or two strap layers). The results showed that the PTMS technique was very effective at enhancing the strength and ductility of the columns. As expected, the use of high volumetric confinement ratios (zero strapping spacing and/or applications with two layers of metal straps) generally led to the highest enhancements. Based on calibration with these test results, the authors proposed a stress-strain model for concrete columns confined with PTMS [Moghaddam et al., 2010b]. Samadi et al. [2012] performed cyclic tests on four substandard lap-spliced RC columns with and without PTMS. Whilst the unconfined control column failed prematurely due to cover splitting and spalling of the concrete cover around the lapped bars, the PTMS-strengthened columns failed in a ductile manner after yielding of the longitudinal reinforcement. Helal [2012] tested four substandard full-scale RC joint specimens strengthened with PTMS under cyclic loading. No stirrups were provided in the joint core

to induce a shear failure in the original bare specimens. After the initial tests, the joints were repaired and subsequently strengthened with PTMS using different strapping layouts and layers. The PTMS technique was proven effective at enhancing the capacity of the strengthened joints by up to 95% compared to the original bare counterparts. Whilst these studies investigated the use of the PTMS technique at the element level, it is necessary to verify its effectiveness at a global level through tests on full-scale RC buildings before this technique can be widely used in practice.

This paper presents the global results of the first three testing Phases of the EU-funded research project BANDIT [Mongabure, 2012]. The main objective of the project was to investigate experimentally the seismic behaviour of a substandard full-scale RC building strengthened with PTMS. The experiments were performed on the AZALEE shaking table at the CEA/EMSI laboratory in Saclay (France), as part of the EU SERIES Programme (Seismic Engineering Research Infrastructures for European Synergies).

2   Experimental programme

The seismic performance of a substandard RC building was investigated through a series of unidirectional full-scale shaking table tests in two orthogonal directions. The building was initially damaged significantly, and then repaired and strengthened with PTMS before additional seismic tests were performed. Phase 1 corresponds to the seismic testing of the bare building in the X direction, and Phases 2 and 3 correspond to the seismic testing of the PTMS-strengthened building in the X and Y directions, respectively. A detailed description of the testing programme is given in the following sections.

2.1   Geometry of the building

The tested structure (see Fig. 2) was a one-bay two-storey frame building regular in plan and elevation, similar to a building tested as part of the EU ECOLEADER programme [Chaudat et al., 2005; Garcia et al., 2010] and built according to substandard construction practices of developing countries. Fig. 3(a) to (c) show details of the general geometry of the building, cross sections of

members and corresponding reinforcement. The building was 4.26×4.26 m in plan and had a constant floor height of 3.30 m, as shown in Fig. 3(a) and (b), respectively. The cross section of the columns was 260×260 mm (Fig. 3(c)). The 1st floor columns were reinforced with eight 14 mm deformed bars, whilst the 2nd floor columns had four 14 mm deformed bars. This resulted in longitudinal reinforcement ratios (ρ_l) of 1.82% and 0.91% for the 1st and 2nd floor columns, respectively. These relatively low ratios are typical of substandard columns. The reduction of longitudinal column reinforcement between floors is a typical construction practice adopted in many developing countries to save material costs. The columns had transverse reinforcement consisting of 6 mm stirrups at 200 mm spacing. The stirrups were closed with 90° bends instead of 135° hooks required by current seismic codes.

In order to examine different beam strengths in the two orthogonal directions, the cross section of the beams was 260×400 mm in the X direction, and 260×300 mm in the Y direction (see Fig. 3(c)). The top and bottom beam reinforcement consisted of four 14 mm bars, resulting in ρ_l values of 0.65% and 0.90% for the beams in the X and Y directions, respectively. Shear reinforcement was provided using 8 mm steel stirrups at 250 mm spacing. Similar to columns, no special measure was taken at the potential plastic hinge zones of the beams. It should be mentioned that the spacing of stirrups in beams and columns of the building was similar to the ECOLEADER building, where such spacing was effective at preventing shear failures in these members.

The top and bottom of the 120 mm thick slabs were reinforced using 10 mm bars spaced at 100 mm centres in both directions (see Fig. 3(c)). Table 1 shows the axial load on columns (N), yield (M_y) and ultimate (M_u) flexural strengths of beams and columns obtained using moment-curvature analysis. The values shown in Table 1 indicate that a strong beam-weak column mechanism is expected to control the behaviour of the building.

To study the effect of beam-column joint detailing on the local and global seismic performance of the building, different types of substandard anchorage details were examined as shown in Fig. 4(a) to (c). For the 1st floor joints, the top beam reinforcement was anchored using a 90° bend in the X direction,

and a hook in the Y direction, respectively (Fig. 4(a) and (b)). To study the effect of short bar anchorage length, the bottom beam reinforcement was anchored into the joints for a length of 220 mm (approximately $16d_b$, where d_b is the bar diameter), with no hooks or bends. This short anchorage length is considered insufficient to develop the yielding capacity of the 14 mm bars according to current design recommendations. For the 2nd floor joints, top and bottom beam reinforcement bars were anchored into the joints for 220 mm in both X and Y directions, as shown in Fig. 4(c). To replicate old substandard construction practices, no transverse stirrups were provided in the joint core. In addition, the longitudinal column bars were lapped over a length $l_b=25d_b=300$ mm just above the joint core, which is considerably less than the required lap splice lengths in high seismic regions (see EN 1998-1:2004 [CEN 2004]). Therefore, significant damage was expected in columns and beam-column joints during the initial tests on the bare building (Phase 1).

In this paper, columns and beam-column joints of the building are identified using an ID code according to their location in plan and elevation. The first letter of the ID represents the type of structural member ("C"=column, "J"=joint), whilst the subsequent digit and letter stand for the axes' intersection at which the member is located in plan. The last digit and letter indicate the floor number and the direction being considered. For instance, the element J1A-2X corresponds to the beam-column joint of the 2nd floor located at the intersection of axes 1 and A, and parallel to the X axis (see Fig. 3(a)).

2.2 Material properties

The building was cast off the shaking table using two batches of ready mixed concrete (one for each floor). To produce vertical slots through the slabs and ease the subsequent installation of the metal straps on the beams, rectangular pieces of expanded polystyrene were placed at the locations shown in Fig. 3(a) prior to casting. Four plastic pipes were also placed vertically in each slab formwork to enable the subsequent clamping of additional masses. Pieces of 1/4 pipes (radius=20 mm) were glued to the corners of the columns' formwork to avoid grinding the sharp corners at the strengthening zones. Though such large radius was not strictly needed for the PTMS, the structure was also strengthened later using externally bonded CFRP sheets, for which sharp corners may be a problem.

The concrete was cured in the formwork for seven days following casting, and then kept under standard laboratory conditions until testing. For each concrete batch, the compressive strength (f_c) and elastic modulus (E_c) were obtained from tests on nine 160×320 mm cylinders according to the CPC 8 guidelines [RILEM, 1994]. The indirect tensile splitting strength (f_{ct}) was determined from tests on twelve 160×320 mm cylinders according to NF EN 12390-6 [AFNOR, 2012]. The flexural strength (f_{cf}) was obtained from four-point bending tests on three prisms of 100×100×500 mm according to NF EN 12390-5 [AFNOR, 2012]. All cylinders and prisms were cast at the same time and cured under the same conditions as the building. Table 2 reports the average results and standard deviations from the tested cylinders and prisms. The shaking table tests started at 119 and 105 days after the cast of the 1st and 2nd floors, respectively.

Due to difficulties in finding low-strength smooth steel bars, the reinforcing steel of the building consisted of deformed bars grade S500 complying with NF A 35-016-1 [AFNOR, 2007]. Compared to low-strength bars, the use of deformed bars S500 is more critical because the joints and columns can be subjected to higher force and bond demands. Table 3 summarises the yield and ultimate strengths obtained from the direct tension tests on three bar samples. Based on previous research by Helal [2012], commercially available high-strength metal straps with nominal cross section 0.8×25 mm and zinc corrosion-resistant surface coating were used for the PTMS strengthening (if necessary, corrosion resistance can be provided by other coatings). The mechanical properties of the straps were obtained from four sample coupons as reported in Table 3. More detailed information about the adopted repairs and strengthening technique is provided in Section 3.2.

2.3 Test setup and instrumentation

2.3.1 Fixity and additional masses

Stiff steel "shoe" supports with high-strength bolts were used to clamp the building rigidly to the shaking table. The column flexural reinforcement was anchored and welded on the base of the "shoes". The welding of these bars was to prevent failure at the column-"shoe" interface during the tests at high seismic intensities as reported by Balsamo et al. [2005]. To simulate additional

permanent and variable loads, three steel plates with a total mass of 13.5 tonnes were bolted underneath the 1st floor slab using post-tensioned high-strength bolts, as shown in Fig. 3(b). One steel plate and one concrete block were clamped to the top of the 2nd floor slab to add a mass of 11.0 tonnes. These additional masses were supported on four half-ball steel bearings at the expected slab inflection points to allow the free deformation of the slabs during the tests (Fig. 3(a)). The steel plates below the 1st floor were initially placed on the shake table and clamped to the slab after moving/fixing the building to the table. Subsequently, the steel plates and concrete blocks were placed on the top of the 2nd floor slab. A similar arrangement was previously used in the ECOLEADER project [Chaudat et al., 2005; Garcia et al., 2010]. The estimated self-weight of the building was 20.4 tonnes. The self-weight and the additional masses produced approximate normalised axial load ratios $v=N/(f_cA_g)$ of 0.05 and 0.03 for the 1st and 2nd floor columns, respectively, where N is the axial load and A_g is the column gross cross sectional area. These relatively low axial load ratios can be justified as substandard structures in developing countries usually have short span lengths.

2.3.2 Seismic record and dynamic identification

An artificial ground motion record based on Eurocode 8 (EC8, EN 1998-1:2004) soil type C spectrum [CEN, 2004] was used as horizontal input. The matching of the input record and EC8 spectra was performed analytically using commercial software (SignalStar by Data Physics). The record length was 30 s, with a frequency range of 0.7-30 Hz. The ground motion record was scaled to apply different levels of peak ground acceleration (PGA). In general, a good matching between the input record spectrum and the table response spectrum was observed for the range of frequencies of interest at all excitation levels. For instance, Fig. 5 compares the spectra for the "EC8" for 5% of critical damping, the "input" record, and the "AZALEE" actual response recorded on the shaking table at PGA=0.35g.

Natural frequencies of the structure were obtained using white noise before and after each test in the X and Y directions. For this purpose, a low intensity excitation (maximum PGA=0.05g) containing a frequency range of 0.5-50 Hz was used. The response recorded at each floor was then used to identify

the natural frequencies of the relevant vibration modes. All data were monitored for 50 s and collected by a data acquisition system at a sampling frequency of 600 Hz.

2.3.3 Test sequence

The testing programme consisted of 17 unidirectional shaking table tests conducted in three Phases according to the sequence shown in Table 4. Phase 1 of the experiments consisted of shake table excitations in the X direction (i.e. parallel to axes 1 and 2 in Fig. 3(a)), ranging from PGA=0.025g to 0.15g. The main objective of these tests was to investigate the seismic performance of the substandard RC structure and produce significant, but repairable damage. The effectiveness of the proposed strengthening technique was investigated in Phase 2 of the project. Damaged elements were repaired and then strengthened using the PTMS technique, and additional shake table tests were conducted using earthquake excitations ranging from PGA=0.05g to 0.35g. In Phase 3, the capacity and seismic performance of the PTMS-strengthened building were assessed in the Y direction by applying additional earthquake excitations with PGA ranging from 0.05g to 0.3g. These tests allowed investigating of the residual resistance of the PTMS-strengthened building in the Y direction after producing damage in the X direction (Phase 2).

2.3.4 Instrumentation

Each floor of the building was instrumented with horizontal displacement and acceleration transducers to monitor the response history during the shaking tests (see Fig. 6). As shown in Fig. 6, two equidistant displacement transducers were fixed on each exterior face of the slabs to identify possible in-plan torsion. The displacement transducers were attached to an external rigid frame to facilitate the measurements and quantify the residual displacements after each test. Relative horizontal displacement between the additional masses and slabs was also measured. A series of 59 strategically placed foil-type electrical resistance strain gauges monitored the strain developed along the reinforcement bars of selected beams, columns and joints at J2A-1X, J2A-2X, J1A-1Y, J1B-1Y and J1A-2Y locations (see Figs. 3 and 4). Additionally, circular targets were glued to columns and slabs in order to measure the building displacements using a stereovision system (see Fig. 6). Further details of this visual monitoring technique are reported in Mongabure [2012].

3   Initial tests and PTMS strengthening

3.1   Phase 1: original bare building

In the first testing Phase, the seismic excitation ranged from PGA=0.025g to 0.15g. The test at a PGA level of 0.15g was halted after approximately 20.0 s due to resonance issues with the shaking table. As some large amplitude cycles of the input record were not applied, the test at PGA=0.15g was repeated to apply the complete duration of the time history.

The first two shake table tests (PGA=0.025 and 0.05g) did not produce significant damage to the bare building. The first cracks appeared at the beam-column joints during the test at a PGA level of 0.10g. At PGA=0.15g, some of the 2nd floor joints experienced severe cracking and concrete spalling. The damage observed in joint J2A-2 suggested that a local failure occurred within this joint during this test. This was confirmed by removing the spalled concrete after the test as shown in Fig. 7(a). The beam reinforcement may have also pulled out from the joint due to the excessive crack widths (>10 mm). However, only narrow diagonal cracks formed at the 1st floor joints at this PGA level (see Fig. 7(b)). This indicates that whilst the 2nd floor joints experienced significant local damage due to the lack of stirrups and inadequate reinforcement detailing, the capacity of the 1st floor joints was not fully developed. Concrete cover splitting also occurred along the spliced longitudinal reinforcement of column C2A-2 (Fig. 7(c)). Horizontal cracks appeared in all 2nd floor columns at the location of the internal steel stirrups. The experiments were halted after the second test at PGA=0.15g to avoid irreparable local damage in the 2nd floor joints and a possible collapse of the 2nd floor.

In this study, an equivalent SDOF model is adopted to calculate the lateral stiffness as the building is low-rise, symmetric and regular in plan and elevation, and therefore the first mode is expected to dominate the response (e.g. Thermou and Pantazopoulou [2011]). Fig. 8 shows the change of lateral structural stiffness (K) of the tested structure at different PGA levels. The lateral stiffness was determined as $K=M(2\pi f_1)^2$, where M is the total mass of the building and f_1 is its fundamental frequency measured after each test. It is shown that, as expected, the lateral stiffness of the building deteriorated rapidly with increasing PGA levels, which is in line with the damage progression

observed during the experiments. After the second test at PGA=0.15g, the residual stiffness of the damaged building was only 30% of its original value (K=2300 vs 7740 kN/m).

3.2   Repairs and PTMS strengthening

3.2.1   Repair of damaged joints

After conducting the tests in Phase 1, the damaged beam-column joints were repaired by:

a) Welding the external bars of the bottom beam reinforcement to the column reinforcement to prevent bar pullout (Fig. 9(a)). To achieve this, short bar segments 20-30 mm long were inserted between the column and beam longitudinal reinforcement bars. This was done in the X direction of the 2nd floor joints only.

b) Replacing damaged and spalled concrete with high-strength repair mortar (Fig. 9(b)), and

c) Injecting cracks with epoxy resin (Fig. 9(c)).

Subsequently, sharp corners at the strengthening zones of joints were rounded off to an approximate radius of 20 mm.

3.2.2   Design of PTMS strengthening

The amount and layout of metal straps used for the PTMS strengthening is based on the principle that metal straps are treated as conventional tensile reinforcement. Based on previous experience from experimental work on columns (Frangou et al. [1995]; Moghaddam et al. [2010a]) and on substandard full-scale joint specimens strengthened with PTMS [Helal, 2012], the straps were post-tensioned to approximately 30-40% of their yield strength. The PTMS strengthening was designed to increase the flexural capacity of the columns, and to enhance the shear capacity of the joints. For illustrative purposes, the shear design of a 1st floor joint (X direction) is given below.

The horizontal shear force demand in the joint (V_{jh}) was computed using force equilibrium according to Eq. (1):

$$V_{jh} = T_b - V_{col} \tag{1}$$

where T_b is the tensile yield force of the top reinforcement of beam and slab, and V_{col} is the column shear force.

Using an effective slab width b_{eff}=600 mm, T_b was determined as 471 kN [Garcia, 2013]. By considering inflection points at the mid-height of the floors (floor height H_c=3300 mm), V_{col} was computed assuming that half of the beam yielding moment (M_{by}=156 kNm, Table 1) was carried by the columns above and below the joint (Eq. (2)):

$$V_{col} = \frac{M_{by}}{H_c} = \frac{156 \times 10^3}{3300} = 47 \quad \text{kN} \tag{2}$$

Thus V_{jh}=471-47=424 kN.

The effect of the PTMS confinement on the joint core shear resistance (V_{cc}) was estimated using Eq. (3) [ASCE, 2007]. The confined concrete compressive strength (f_{cc}) due to the horizontal straps was calculated using Moghaddam et al. [2010b] model. Two-layered metal straps spaced at s=50 mm centres and tensioned to 35% of their yield strength are used, resulting in a value f_{cc}=36.3 MPa. A shear strength factor γ=0.083×8=0.66 for exterior joints without internal shear reinforcement was adopted according to the ASCE/SEI 41-06 guidelines [ASCE, 2007].

$$V_{cc} = \gamma A_j \sqrt{f_{cc}} = (0.66)(260 \cdot 260)\sqrt{36.3} = 270 \quad \text{kN} \tag{3}$$

where A_j is the effective horizontal joint area.

The shear resistance provided by the horizontal metal straps (V_{sh}) was then calculated using conventional design principles and considering the straps as additional shear reinforcement (Eq. (4)):

$$V_{sh} = \frac{A_v f_y d_c}{s} = \frac{(2 \cdot 0.8 \cdot 25)(982)(228)}{50} = 180 \quad \text{kN} \tag{4}$$

where A_v is the cross-sectional area of the steel straps and d_c is the effective depth of the column.

The proposed PTMS layout was thus adequate to sustain the design shear force demand in the joint ($V_{cc}+V_{sh}>V_{jh}$).

3.2.3 Installation of PTMS

All columns and joints were strengthened locally using PTMS to increase their capacity. The metal straps were installed progressively, as described below and shown in Figs. 10 and 11.

1. First, six 10 mm thick anchor steel plates were fixed to the columns, beams and top of 2nd floor slab using high-strength M12×120 mm bolts inserted in holes prefilled with epoxy adhesive mortar. After the adhesive set, the plates were positioned and partially tightened with nuts and washers leaving a small gap of approximately 1 mm between the plates and the concrete faces, which was necessary to secure the 2 layer metal straps (see Fig. 10(c)). The diameter of the high-strength bolts and dimensions of the steel plates were conservatively selected to resist the shear force corresponding to the nominal tensile strength of the metal straps.

2. Next, nine horizontal straps at 50 mm spacing were placed at column ends to provide confinement and increase their shear strength.

3. One layer of straps was inserted in the pre-formed slots of the slabs to confine the beam ends and also increase their shear capacity.

4. Based on the calculations presented in the previous section, eight straps (2 layers each) were installed parallel to the longitudinal beams axes (i.e. horizontally) at 50 mm centres to provide confinement to the beam-column joint. These straps were anchored around the steel plates as shown in Fig. 10(c). Due to the different beam depths in the X and Y directions, an additional anchorage plate was placed at the interior face of the deeper beams as shown in Fig. 11(b).

5. Six straps (2 layers each) were provided along the outer faces of the columns (parallel to the column axis) to enhance their flexural capacity. For the 2nd floor joints, the six straps were bent at 90° at the slab edges and secured to steel plates located on the top of the 2nd floor slab as shown in Fig.

10(a). Afterwards, the nuts of the bolts securing the steel plates were tightened by hand using a spanner to prevent the loss of prestressing in the straps.

6. Finally, 1 layer of confinement straps was placed around beams and columns to prevent excessive buckling of the horizontal and longitudinal straps installed at stages 4 and 5.

All straps were fastened using "push type" seals of 25 mm length (see seals in Fig. 1) to maintain the tensioning force. Fig. 11(c) and (d) show typical beam-column joints after the PTMS strengthening. As can be seen, the metal strapping provided a confining grid around the beam-column joints and columns ends. The total strapping time for each joint varied from 2 to 3 hrs, which demonstrates the speed of application of the proposed strengthening technique. In addition, the added weight of the steel plates and metal straps was considered negligible compared to the total weight of the building. The amount of steel used in the PTMS strengthening of all joints was approximately 220 kg.

4 PTMS tests and discussion

4.1 Phase 2: PTMS-strengthened building (X direction)

The seismic excitation applied to the building after repair and PTMS strengthening ranged from PGA=0.05g to 0.35g (Table 4). In general, as the metal straps covered much of the concrete surfaces, damage at the joints could not be observed during the tests. However, metallic sounds during tests (especially after a PGA=0.15g) indicated that the metal straps were tensioning considerably at the joints and columns. After the tests were halted, a thorough inspection revealed that no apparent damage occurred at the straps or steel plates. Overall, the metal straps maintained the post-tensioning force, with the exception of a few longitudinal straps placed along the columns of the 1st floor joints. This loss of force can be attributed to the partial shearing off of some "push type" metal seals, which had poor bearing resistance to start with. Significant cracking was also evident in the beam-column joints, particularly at J1A-1X, J1A-2X, J2A-1X and J2A-2X locations. The tests show that whilst the 2nd floor of the bare building (in Phase 1) was approaching collapse at a seismic intensity PGA=0.15g, the PTMS-strengthened building (in Phase 2) sustained a PGA=0.35g earthquake without extensive

damage or compromising the global stability. Maximum relative displacement between the additional masses and slabs was 1 mm at PGA 0.35g. Due to the arrangement and detailing of the mass supports (see Fig. 3), only a fraction of the 2nd floor lateral inertia force was transferred as axial loads to the steel bearings (i.e. the floor slabs were not subjected to additional bending moments). Therefore, the effect of vertical mass eccentricity was considered to be negligible.

The damage observed in the building in Phase 2 indicates that the repairs and PTMS strengthening intervention enhanced considerably the shear capacity of the 2nd floor joints, preventing their premature failure. As a consequence, seismic force demands redistributed among other structural members and the 1st floor joints were subjected to higher forces, leading to significant cracking. This implies that the PTMS strengthening intervention exploited better the available members' capacities and led to a more uniform damage distribution over the height of the structure. A uniform damage distribution commonly leads to less overall structural damage and better seismic performance under strong earthquakes [e.g. Hajirasouliha et al., 2012].

Fig. 8 indicates that the repairs and PTMS strengthening restored the stiffness of the building from K=2300 kN/m (damaged) to 4820 kN/m (after repair). The latter stiffness is similar to that of the bare building after the test PGA=0.05g, which corresponds to a post-cracked elastic stage. Fig. 8 also shows that at a PGA=0.15g, the stiffness degradation of the building was 70% in Phase 1 (from 7740 to 2300 kN/m) and 21% in Phase 2 (from 4820 to 3830 kN/m). This implies that the adopted repairs and strengthening technique were very effective at controlling the stiffness degradation of the building, which is important in seismic strengthening design.

4.2   Phase 3: PTMS-strengthened building (Y direction)

In this Phase, the PTMS strengthened building was subjected to earthquake excitations ranging from PGA=0.05 to 0.30g in the Y direction. The Y direction was weaker than the X direction due to the smaller depth of the beams. No significant damage was observed in the metal straps during the tests. However, a visual inspection after the removal of the metal straps and spalled concrete confirmed that the beam-column joints experienced extensive cracking, as shown in Fig. 12(a) and (b). Nonetheless,

the PTMS technique has proven extremely effective at maintaining the integrity of the joints. Whilst the relatively high intensity of the seismic excitation produced additional damage to the building, none of the structural elements showed evidence of potential failure. The good performance observed in the Y direction also suggests that the welding of the beam and column bars (performed in the X direction) may not be necessary for rapid strengthening applications. However, in general the welding of bars is expected to enhance the seismic performance of buildings. Fig. 13 compares the stiffness of the building in the Y direction during Phase 3 with the stiffness values at the beginning of Phases 1 and 2 in the same direction. The results indicate that, due to damage accumulation produced by the shaking in the X direction, the initial stiffness of the building in Phase 3 reduced by 62% and 41% in comparison to the bare building (K_{iY}=6600 kN/m, beginning of Phase 1) and after the PTMS strengthening (K=4260 kN/m, beginning of Phase 2), respectively. Moreover, although no significant damage was observed during the tests in Phase 3, the residual stiffness of the building decreased by 43% with reference to its initial value at the start of Phase 3 (K=1430 vs 2510 kN/m, respectively). It should be mentioned that although the building was clearly capable of sustaining seismic excitations at higher PGA intensities and the majority of the straps were intact, the tests were halted after a PGA level of 0.30g to evaluate the local damage at the joints and the global condition of the structure. Moreover, structural damage had to be maintained within repairable limits as further shaking table tests were planned on the building.

4.3 Time-history results

Fig. 14 shows displacement time-history of the 1st and 2nd floors for the last test performed in each testing Phase. It is shown that the 2nd floor exhibited higher lateral displacement (up to 160%) compared to the 1st floor in all three tests. Fig. 14 shows that residual displacements at the end of Phases 2 and 3 were very small (approximately 2-3 mm), which confirms the effectiveness of the PTMS intervention at controlling damage and maintaining the building stability. The test in Phase 1 was halted after approximately 32 s (see Fig. 14 (a)) to prevent the possible collapse of the 2nd floor, and therefore, residual displacements were not measured. In general, readings from the equidistant

displacement transducers fixed on the exterior faces of the slabs were very similar, which indicates that in-plan torsion was negligible during all three testing Phases.

Fig. 15 compares strain time-history readings from gauges fixed on the bottom beam reinforcement of the 1st floor (gauges marked with an asterisk in Fig. 4). As shown in Fig. 15 (a), elastic strains of 300-400 $\mu\varepsilon$ accumulated during the initial tests in Phase 1 due to damage at the bar-concrete interface. In comparison, very small strains (120 $\mu\varepsilon$) accumulated during Phases 2 and 3, which indicates that most of the seismic force demand was taken by the metal straps rather than by the internal reinforcement. The readings from the strain gauges fixed on the reinforcing bars indicated that no yielding occurred in beams or columns.

4.4   Global damage index

It has been suggested that the change in structural period is an appropriate parameter to assess the global damage experienced by buildings subjected to earthquakes (DiPasquale and Çakmak [1988]; DiPasquale et al. [1990]; Zembaty et al. [2006]). Therefore, this study adopts the global damage index (DI) proposed by DiPasquale et al. [1990] to assess quantitatively the structural damage of the tested building at different PGA levels. The global damage index is defined as $DI=1-(T_i/T_f)^2$, where T_i and T_f are the natural periods of the building in initial undamaged condition and after an earthquake, respectively. Accordingly, a DI value of zero implies no damage to the building, whereas a DI value of 1.0 represents the theoretical collapse of the structure. Fig. 16 shows the global DIs calculated for each shaking table test using the formula above. The values T_i and T_f were taken as the initial periods of the bare undamaged building and the periods after each test, respectively. It should be mentioned that any global damage index should be calibrated before it can be directly associated to a specific damage state. However, in this study the global damage index is used mainly to compare quantitatively the global structural damage experienced by the building during different testing Phases.

Phase 1. The results in Fig. 16 indicate that the bare building was not very close to its theoretical collapse point at a PGA=0.15g (DI=0.70), as also suggested by the experimental observations.

17

Nonetheless, the experimental evidence showed severe local damage, which is not very easy to capture using a global damage index.

Phase 2. Fig. 16 shows that at a PGA=0.15g, the PTMS-strengthened building exhibited a *DI* of only 0.51, which indicates a damage reduction of 27% compared to the bare building (Phase 1). It is also shown that the damage of the strengthened building at PGA=0.30g (*DI*=0.70) was identical to that obtained at a considerably lower PGA=0.15g in the bare building and no local damage was observed. Although the tests in Phase 2 were stopped at a relatively high PGA=0.35g, the *DI* value only reached 0.78 (without severe local damage) and could potentially resist higher PGAs.

Phase 3. Despite the significant damage accumulated at the start of this testing phase (*DI*=0.64) due to shaking in the X direction, the PTMS-strengthened building in the Y direction (Phase 3) showed similar levels of damage as the bare building at PGA=0.15g (*DIs*=0.69 and 0.70, respectively) tested in the X direction (stronger direction).

Based on the results, it is clear that global damage was well controlled in the PTMS-strengthened building, particularly at higher levels of PGA. This indicates that the PTMS-strengthening technique was very effective at sustaining structural stability and delaying a potential collapse.

4.5 Performance levels

In performance-based design methods, design criteria are expressed in terms of achieving specific performance targets during a design level earthquake. Performance targets could be satisfied by controlling the level of structural and non-structural damage. Current guidelines for seismic rehabilitation of existing buildings such as ASCE/SEI 41-06 [ASCE, 2007] place limits on acceptable values of inter-storey drift ratios implying that exceeding these limits is a violation of a performance objective. According to ASCE/SEI 41-06, maximum transient drift ratios of 1%, 2% and 4% correspond to Immediate Occupancy (IO), Life Safety (LS), and Collapse Prevention (CP) performance levels, respectively.

Phase 1. Fig. 17 shows the maximum inter-storey drift ratios (δ) of the 1st and 2nd floors obtained for each shaking table test. The results indicate that the 1st and 2nd floors of the bare building had similar drift ratios at PGA levels of 0.025g, 0.05g and 0.10g. However, when the building was subjected to a PGA=0.15g, the 2nd floor drift value was 100% higher than that of the 1st floor (δ=1.69% vs 0.82%). This sharp increase of the drift ratio can be attributed to the significant local damage of the beam-column joints at the 2nd floor, as observed in the experiments.

Phase 2. It is shown in Fig. 17 that the drift ratios of the bare and PTMS-strengthened buildings were very similar at a PGA=0.05g (0.29% vs 0.30%). At a PGA level of 0.10g, the drift ratios of the 1st and 2nd floors of the strengthened building (Phase 2) were respectively 33% and 25% higher than the corresponding ratios measured on the bare building (Phase 1). While the 2nd floor of the bare structure was within LS level at a PGA=0.15g (δ=1.69%) due to the local damage, the critical drift ratio of the strengthened building was very close to the IO performance level (δ=1.14%), which is consistent with the experimental observations. In general, the local repairs and PTMS strengthening of the joints were very effective at reducing the critical drift of the 2nd floor (i.e. critical storey). As discussed in Section 4.1, this led to a more uniform distribution of damage in the structure.

Despite the relatively high seismic excitation applied during the last test on the strengthened building (PGA=0.35g), the maximum drifts of both floors were at the early stages of CP. This implies that the adopted repair and PTMS strengthening strategy was very effective at improving the seismic performance of the building by reducing structural deterioration at the 2nd floor and critical inter-storey drifts.

Phase 3. The effectiveness of the PTMS strengthening is emphasised by comparing the maximum inter-storey drifts of the strengthened building in the X and Y directions (Fig. 17). Although no rehabilitation was done after Phase 2, similar maximum inter-storey drifts were observed during the shaking table tests in the X and Y directions up to PGA=0.25g (Phases 2 and 3, respectively).

Fig. 17 shows that the maximum drift ratios of the PTMS-strengthened structure in both X and Y directions were within the CP performance level. In particular, the 1st floor was very close to LS level.

This shows that despite the damage produced by the earthquakes applied in the X direction (Phases 1 and 2), the building was capable of resisting additional earthquakes in the Y direction (Phase 3).

Based on the results of this study, it is concluded that the PTMS technique is a feasible and very effective for quick post-earthquake strengthening of substandard RC buildings. Owing to the low material costs and ease of installation, this technique is especially suitable for structures in developing countries. The results of subsequent testing phases of this research programme, which pushed the building to 3D shaking of PGA=0.6g, will be presented in future publications.

5   Summary and conclusions

This paper presents the results of the first three testing phases of the EU-funded project BANDIT. The project investigated the effectiveness of a novel strengthening technique using Post-Tensioned Metal Straps (PTMS) through shaking table tests on a full-scale RC building. The building had inadequate reinforcement detailing in columns and beam-column joints to simulate typical deficiencies of substandard existing buildings in developing countries. From the results presented in this study, the following conclusions can be drawn:

1) The capacity of the substandard bare building was limited by the premature local failure of the beam-column joints at the 2nd floor. Following various levels of seismic excitation, the joints and columns at the 1st floor experienced limited damage. The damage produced during the shaking table tests in the X direction (Phase 1) reduced the initial stiffness of the bare building by 70%. The tests were halted at a PGA level of 0.15g to avoid excessive damage and a possible collapse of the 2nd floor.

2) The PTMS strengthening technique was shown to be easy to apply and was done without the use of adhesives, sophisticated equipment or materials. The amount of steel straps used for the building did not exceed 250 kg, which confirms that the major costs of strengthening come from labour.

3) The repairs and local PTMS strengthening of columns and joints after initial tests were effective at restoring the stiffness of the building to a post-cracked stage. The results show that the adopted repair and PTMS strengthening solutions reduced the stiffness degradation of the building from 70% to 21% at PGA=0.15g.

4) The repairs and PTMS strengthening enhanced the capacity of the severely deteriorated 2nd floor beam-column joints. This resulted in a more uniform damage distribution and better exploitation of the available capacity in the structure. While the bare structure reached a critical level of damage at PGA=0.15g, the PTMS-strengthened building resisted seismic shaking up to PGA=0.35g without compromising its stability.

5) The local rehabilitation and PTMS strengthening of the columns and joints resulted in a considerable reduction (up to 30%) of the inter-storey drift ratio of the 2nd floor at PGA=0.15g. Following strengthening, the seismic performance of the bare building at the 2nd floor improved from near Collapse Prevention to near Immediate Occupancy performance level.

6) The PTMS-strengthened building was clearly capable of resisting additional seismic excitations up to PGA=0.3g in the Y direction, after the damage produced by a series of earthquakes in the X direction. The building remained within the Collapse Prevention performance level and its stability was never compromised. On the basis of the above discussion, it can be concluded that the low-cost and simple strengthening method is very effective for rapid post-earthquake strengthening of substandard RC structures, and it is especially suitable for applications in developing countries.

References

AFNOR [2007] "NF A 35-016-1 Aciers pour beton arrne - Aciers soudables a verrous Partie1: Barres et couronnes," Association Française de Normalisation, France.

AFNOR [2012] "NF EN 12390-5 Essais pour béton durci - Partie 5: résistance à la flexion sur éprouvettes," Association Française de Normalisation, France.

AFNOR [2012] "NF EN 12390-6 Essais pour béton durci - Partie 6: détermination de la résistance en traction par fendage d'éprouvettes," Association Française de Normalisation, France.

Akguzel, U. and Pampanin, S. [2010] "Effects of variation of axial load and bi-directional loading on seismic performance of GFRP retrofitted reinforced concrete exterior beam-column joints," Journal of Composites for Construction, 14(1), 94-104.

Al-Salloum, Y.A., Almusallam, T.H., Alsayed, S.H. and Siddiqui, N.A. [2011] "Seismic behavior of as-built, ACI-complying, and CFRP repaired exterior RC beam-column joints," Journal of Composites for Construction, 15(4), 522-534.

Alsayed, S.H., Al-Salloum, Y.A., Almusallam, T.H. and Siddiqui, N.A. [2010] "Seismic response of FRP-upgraded exterior RC beam-column joints," Journal of Composites for Construction, 14(2), 195-208.

Antonopoulos, C.P. and Triantafillou, T.C. [2003] "Experimental investigation of FRP-strengthened RC beam-column joints," Journal of Composites for Construction, 7(1), 39-49.

ASCE [2007] "ASCE/SEI 41-06 Seismic Rehabilitation of Existing Buildings," American Society of Civil Engineers, Reston, VA.

Balsamo, A., Colombo, A., Manfredi, G., Negro, P. and Prota, A. [2005a] "Seismic behavior of a full-scale RC frame repaired using CFRP laminates," Engineering Structures, 27(5), 769-980.

Balsamo, A., Manfredi, G., Mola, E., Negro, P. and Prota, A. [2005b] "Seismic rehabilitation of a full-scale structure using GFRP laminates," ACI Structural Journal, SP230-75, 1325-1344.

Beres, A., Pessiki, S.P., White, R.N. and Gergely, P. [1996] "Implications of experiments on the seismic behavior of gravity load designed RC beam-to-column connections," Earthquake Spectra, 12(2), 185-198.

Biddah, A., Ghobarah, A. and Aziz, T.S. [1997] "Upgrading of nonductile reinforced concrete frame connections," Journal of Structural Engineering-ASCE, 123(8), 1001-1010.

CEN (2004) "EN 1992-1-1 Eurocode 2 - Design of Concrete Structures Part 1-1: General Rules and Rules for Buildings," Comité Européen de Normalisation, Lausanne, Switzerland.

CEN [2004] "EN 1998-1:2004 Eurocode 8 - Design of Structures for Earthquake Resistance Part 1: General rules, seismic actions and rules for buildings," Comité Européen de Normalisation, Lausanne, Switzerland.

Chaudat, T., Garnier, C., Cvejic, S., Poupin, S., Le Corre, M. and Mahe, M. [2005] "ECOLEADER Project no. 2: seismic tests on a reinforced concrete bare frame with FRP retrofitting-Tests Report," Report SEMT/EMSI/RT/05-006/A, Saclay, France.

Corazao, M. and Durrani, A.J. [1989] "Repair and Strengthening of beam to-column connections subjected to earthquake loading," Technical Report NCEER-89-0013, State University of New York, Buffalo.

Della Corte, G., Barecchia, E. and Mazzolani, F.M. [2006] "Seismic upgrading of RC buildings by FRP: full-scale tests of a real structure," Journal of Materials in Civil Engineering, 18(5), 659-669.

Di Ludovico, M., Prota, A., Manfredi, G. and Cosenza, E. [2008] "Seismic strengthening of an under-designed RC structure with FRP," Earthquake Engineering and Structural Dynamics, 37(1), 141-162.

DiPasquale, E. and Çakmak, A.S. [1988] "Identification of the serviceability limit state and detection of seismic structural damage," Report NCEER-88-0022, National Centre for Earthquake Engineering Research, State University of New York at Buffalo, NY.

DiPasquale, E., Ju, J., Askar, A. and Çakmak, A.S. [1990] "Relation between global damage indices and local stiffness degradation," Journal of Structural Engineering-ASCE, 116(5), 1440-1456.

Frangou, M. [1996] "Strengthening of concrete by lateral confinement," Ph.D. thesis, Dept. of Civil and Structural Engineering, The University of Sheffield, UK.

Frangou, M., Pilakoutas, K. and Dritsos, S. [1995] "Structural repair/strengthening of RC columns," Construction and Building Materials, 9(5), 259-266.

Garcia, R [2013] "Seismic strengthening of substandard RC structures using external reinforcement," Ph.D. thesis, Dept. of Civil and Structural Engineering, The University of Sheffield, UK.

Garcia, R., Hajirasouliha, I. and Pilakoutas, K. [2010] "Seismic behaviour of deficient RC frames strengthened with CFRP composites," Engineering Structures 32(10), 3075-3085.

Gergely, J., Pantelides, C.P. and Reavely, L.D. [2000] "Shear strengthening of RCT-joints using FRP composites," Journal of Composites for Construction, 4(4), 198-205.

Ghobarah, A. and El-Amoury, T. [2005] "Seismic rehabilitation of deficient exterior concrete frame joints," Journal of Composites for Construction, 9(5), 408-416.

Ghobarah, A. and Said, A. [2001] "Seismic rehabilitation of beam-column joints using FRP laminates," Journal of Earthquake Engineering, 5(1), 113-129.

Ghobarah, A. and Said, A. [2002] "Shear strengthening of beam-column joints," Engineering Structures, 24(7), 881-888.

Ghobarah, A., Aziz, T.S. and Biddah, A. [1996] "Seismic rehabilitation of reinforced concrete beam-column connections," Earthquake Spectra, 12(4), 761-780.

Granata, P.J. and Parvin, A. [2001] "An experimental study on Kevlar strengthening of beam-column connections," Composite Structures, 53(2), 163-171.

Hajirasouliha, I., Asadi, P. and Pilakoutas, K. [2012] "An efficient performance-based seismic design method for reinforced concrete frames," Earthquake Engineering and Structural Dynamics, 41(4), 663-679, 2012.

Helal, Y. [2012] "Seismic strengthening of deficient RC elements using PTMS," Ph.D. thesis, Dept. of Civil and Structural Engineering, The University of Sheffield, UK.

Ilki, A., Bedirhanoglu, I., and Kumbasar, N. [2011] "Behavior of FRP-retrofitted joints built with plain bars and low-strength concrete," Journal of Composites for Construction, 15(3), 312-326.

Karayannis, C.G. and Sirkelis, G.M. [2008] "Strengthening and rehabilitation of RC beam-column joints using carbon-FRP jacketing and epoxy resin injection," Earthquake Engineering and Structural Dynamics, 37(5),769-790.

Karayannis, C.G., Chalioris, C.E. and Sideris, K.K. [1998] "Effectiveness of RC beam-column connection repair using epoxy resin injections," Journal of Earthquake Engineering, 2(2), 217-240.

Karayannis, C.G., Chalioris, C.E. and Sirkelis, G.M. [2008] "Local retrofit of exterior RC beam-column joints using thin RC jackets - An experimental study," Earthquake Engineering and Structural Dynamics, 37(5), 727-746.

Le-Trung, K., Lee, K., Lee, J. and Sungwoo, W. [2010] "Experimental study of RC beam-column joints strengthened using CFRP composites," Composites Part B: Engineering, 41(1), 76-85.

Moghaddam, H., Samadi, M., Pilakoutas, K. and Mohebbi, S. [2010a] "Axial compressive behavior of concrete actively confined by metal strips; part A: experimental study," Materials and Structures, 43(10), 1369-1381.

Moghaddam, H., Samadi, M. and Pilakoutas, K. [2010b] "Compressive behavior of concrete actively confined by metal strips; part B: analysis," Materials and Structures, 43(10), 1383-1396.

Mongabure, P. [2012] "BANDIT program: Seismic Tests on a Reinforced Concrete Frame with Post-Tensioned Metal Strips Retrofitting - Final Report," SERIES Programme, Seismic Engineering Research Infrastructures for European Synergies, available at www.series.upatras.gr/CEA_project1.

Pantelides, C.P. and Gergely, J. [2008] "Seismic retrofit of reinforced concrete beam column T-joints in bridge piers with FRP composite jackets," SP-258: Seismic Strengthening of Concrete Buildings Using FRP Composites (in CD-ROM), 1-18.

Parvin, A., Altay, S., Yalcin, C. and Kaya, O. [2010] "CFRP rehabilitation of concrete frame joints with inadequate shear and anchorage details," Journal of Composites for Construction, 14(1), 72-82.

Pinto, A.V., Verzeletti, G., Molina, J., Varum, H., Pinho, R. and Coelho, E. [2002] "Pseudodynamic tests on non-seismic resisting RC frames (bare and selective retrofit frames)," Report EUR 20244, JRC-IPSC, Ispra, Italy.

RILEM [1994] "RILEM Recommendations for the Testing and Use of Constructions Materials - CPC 8 Modulus of elasticity of concrete in compression 1975," E & FN SPON, pp. 25-27.

Said, A.M. and Nehdi, N.L. [2004] "Use of FRP for RC frames in seismic zones: Part I. Evaluation of FRP beam-column joint rehabilitation techniques," Applied Composite Materials, 11(4), 205-226.

Samadi, M., Moghaddam, H. and Pilakoutas, K. [2012] "Seismic retrofit of RC columns with inadequate lap-splice length by external post-tensioned high-strength strips," Proc. of the 15th World Conference on Earthquake Engineering, Lisbon, Portugal, (in USB).

Sasmal, S., Ramanjaneyulu, K., Novák, B., Srinivas, V., Kumar, K.S., Korkowski, C., Roehm, C., Lakshmanan, N. and Nagesh, R.I. [2011] "Seismic retrofitting of nonductile beam-column sub-assemblage using FRP wrapping and steel plate jacketing," Construction and Building Materials, 25(1), 175-182.

Sezen, H. [2012] "Repair and strengthening of reinforced concrete beam-column joints with fiber-reinforced polymer composites," Journal of Composites for Construction, 16(5), 499-506.

Thermou, G.E. and Pantazopoulou, S.J. [2011] "Assessment indices for the seismic vulnerability of existing R.C. buildings," Earthquake Engineering and Structural Dynamics, 40(3), 293-313.

Tsonos, A.G. [2008] "Effectiveness of CFRP-jackets and RC-jackets in post-earthquake and pre-earthquake retrofitting of beam-column subassemblages," Engineering Structures, 30(3), 777-793.

Tsonos, A.G. [2010] "Performance enhancement of R/C building columns and beam-column joints through shotcrete jacketing," Engineering Structures, 32(3), 726-740.

Zembaty, Z., Kowalski, M. and Pospisil S. [2006] "Dynamic identification of an RC frame in progressive states of damage," Engineering Structures, 28(5), 668-681.

TABLES

Table 1. Beam and column strengths

	N (kN)	M_y (kNm)	M_u (kNm)
Column 2nd floor	52	38	41
Column 1st floor	110	63	77
Beams X direction (positive)	-	111	127
Beams X direction (negative)[a]	-	156	167
Beams Y direction (positive)	-	79	88
Beams Y direction (negative)[a]	-	108	113

[a] Effective tension flange computed according to EN 1992-1-1 [CEN, 2004]

Table 2. Properties of concrete used to cast the building

	1st floor	2nd floor
Compressive strength, f_c (MPa)	30.7 (1.56)	24.6 (2.03)
Indirect tensile strength, f_{ct} (MPa)	2.67 (0.38)	2.28 (0.22)
Flexural strength, f_{cf} (MPa)	3.60 (0.26)	3.83 (0.32)
Elastic modulus, E_c (GPa)	24.3 (1.30)	21.2 (1.16)

Note: standard deviations are shown in brackets

Table 3. Mechanical properties of steel reinforcement and metal straps

Nominal diameter, d_b (mm)	Ø6	Ø8	Ø10	Ø14	Strap 0.8×25 mm
Yield strength, f_y (MPa)	574 (6)	544 (12)	513 (4)	526 (8)	982 (11)
Tensile strength, f_u (MPa)	604 (9)	572 (9)	587 (9)	616 (2)	1100 (22)
Yield strain, ε_y (%)	0.28	0.26	0.25	0.26	0.43
Elongation at max. force, ε_u (%)	3.0 (0.9)	3.3 (0.6)	6.8 (1.5)	8.0 (2.3)	4.60 (0.5)
Elastic modulus, E_s (%)	207	209	202	201	230

Note: standard deviations are shown in brackets

Table 4. Test sequence and building condition for shaking table tests

Phase	Test direction and condition	PGA (g)	1st mode T_1 (s)	2nd mode T_2 (s)
1	X - Bare building	Undamaged	0.48	0.18
		0.025	0.53	0.20
		0.05	0.60	0.22
		0.10	0.68	0.25
		0.15[a]	0.88	0.29
2	X - Repaired and PTMS-strengthened building	Initial	0.61	0.20
		0.05	0.64	0.21
		0.10	0.67	0.22
		0.15	0.68	0.23
		0.20	0.75	0.23
		0.25	0.78	0.26
		0.30	0.88	0.26
		0.35	1.01	0.27
3	Y - PTMS-strengthened building[b]	Damaged	0.84	0.27
		0.05	0.86	0.27
		0.10	0.93	0.27
		0.15	0.93	0.28
		0.20	0.97	0.29
		0.25	1.08	0.29
		0.30	1.11	0.30

[a] After this test, cracks were resin-injected and damaged concrete replaced with high-strength epoxy mortar. PTMS were subsequently installed.
[b] In Y direction: T_1=0.52 s in undamaged condition (start of Phase 1); T_1=0.65 s after repairs and PTMS strengthening (start of Phase 2).

FIGURES

"Push type" seals

Strapping tool
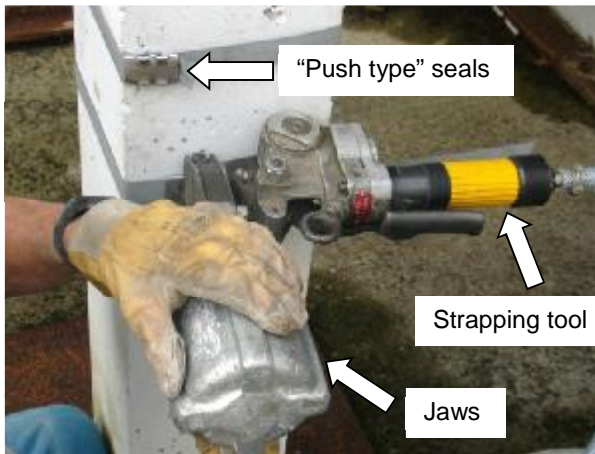
Jaws

Fig. 1. Strapping tool and clamping jaws used for the PTMS strengthening technique

Fig. 2. General view of BANDIT building in bare condition
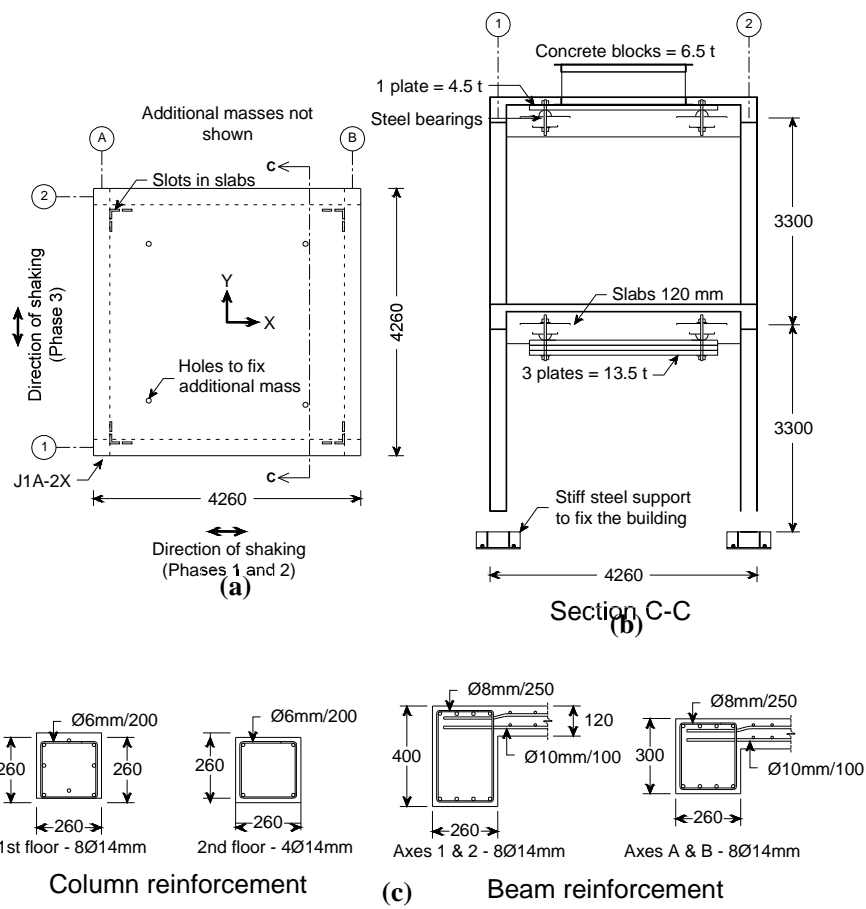
Fig. 3. Geometry of tested building in (a) plan and (b) elevation; (c) reinforcement details of members
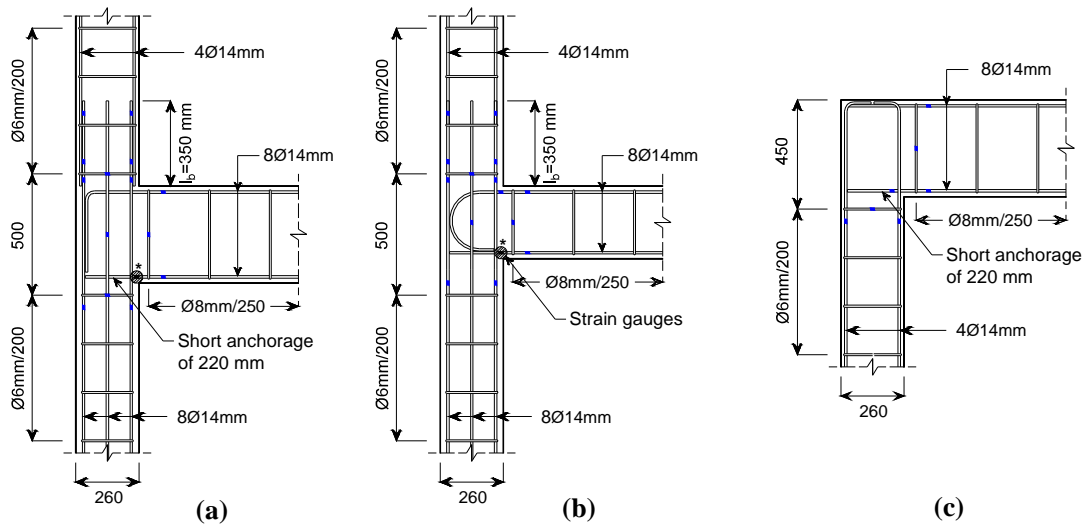
Fig. 4. Detailing of columns and beam-column joints at (a) 1st floor X direction; (b) 1st floor Y direction; and (c) 2nd floor, X and Y directions
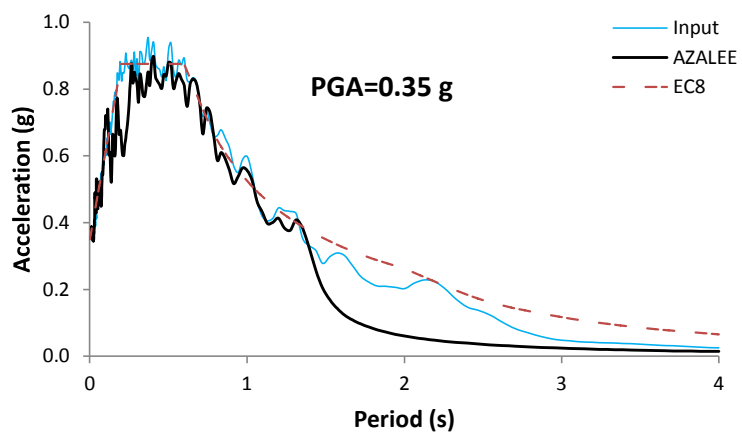
Fig. 5. Matching of response spectra input record and response of shake table (PGA=0.35g)
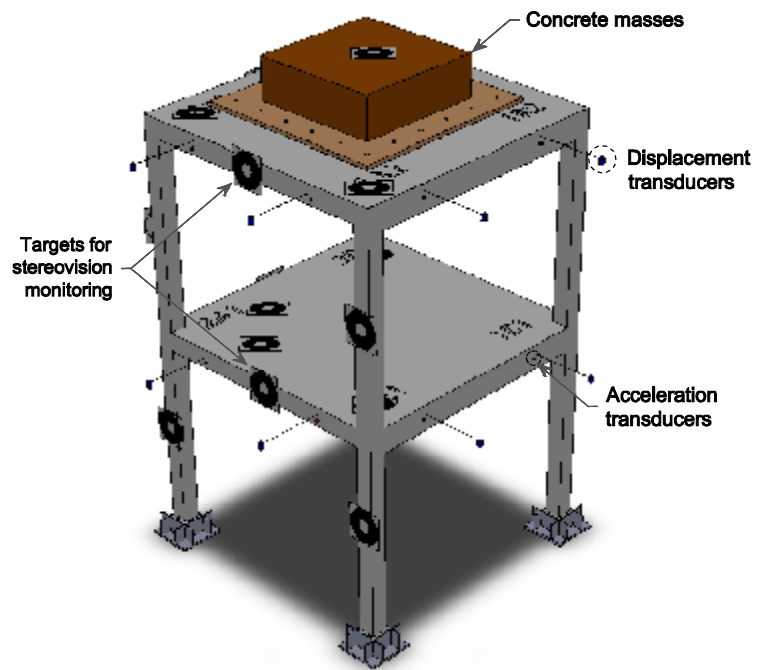
Fig. 6. Instrumentation of BANDIT building
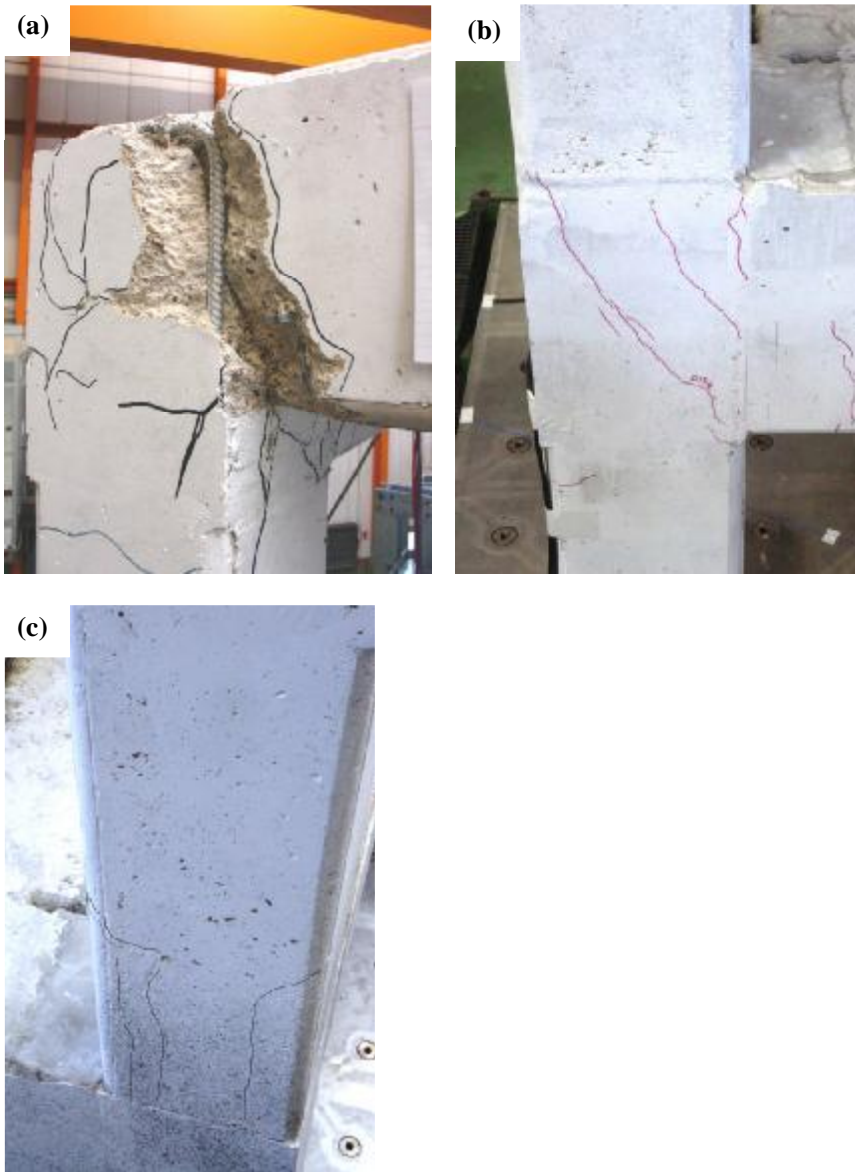
Fig. 7. Damage in beam-column joints and columns after Phase 1: (a) J2A-2Y, (b) J1A-1X, (c) concrete splitting along lapped flexural reinforcement of C2A-2X
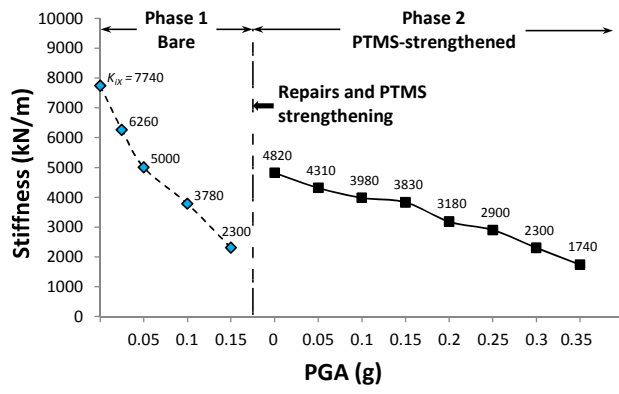
Fig. 8. Lateral stiffness degradation, Phases 1 and 2 (X direction)
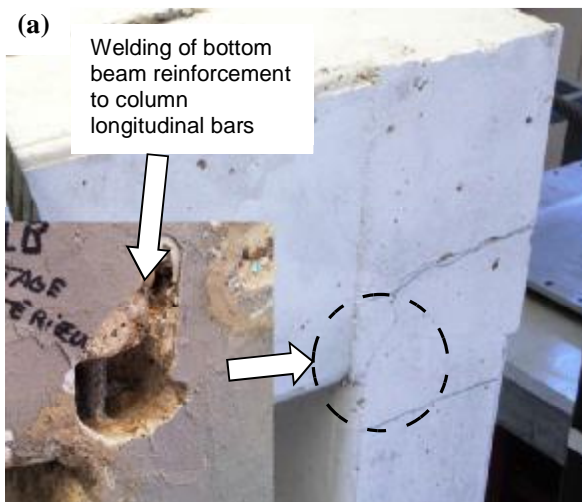
Fig. 9. Repairs after Phase 1: (a) welding of external beam bars to column bars, (b) mortar repair at J2B-2 and injection ports for crack injection, (c) crack injection in progress
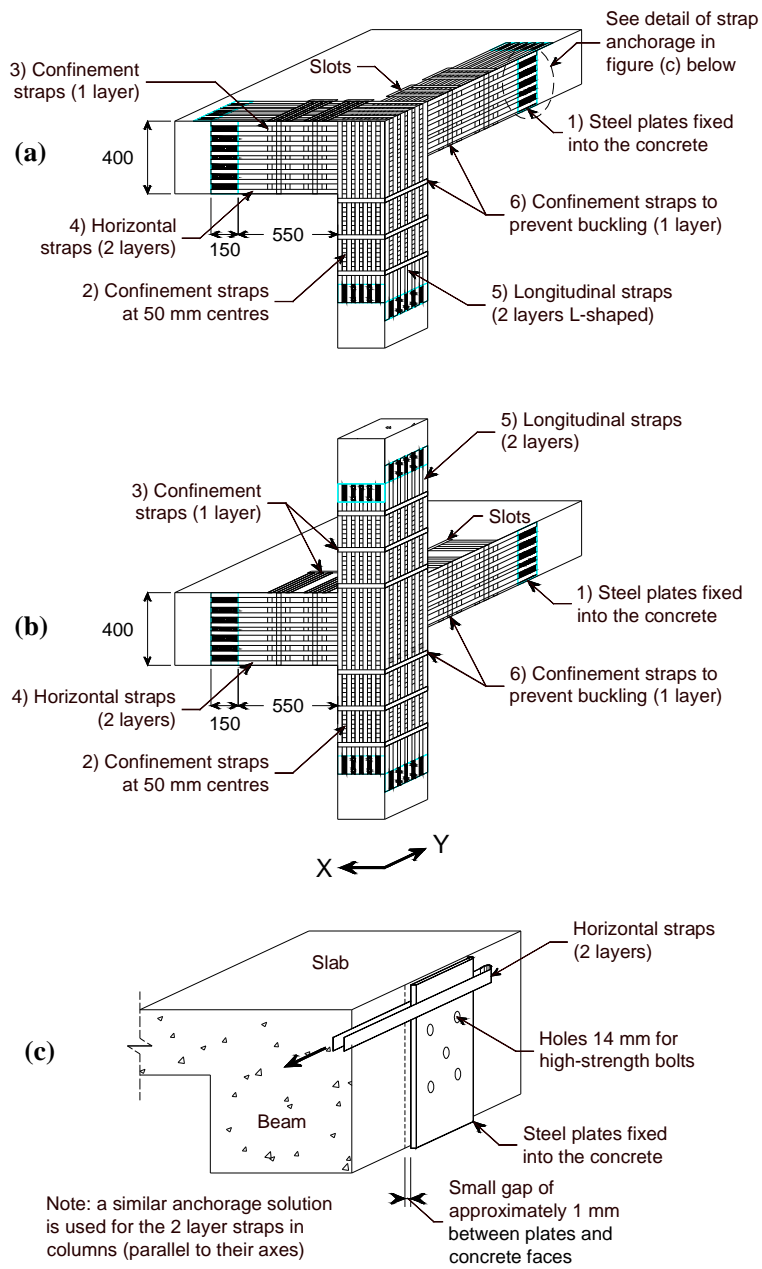
Fig. 10. Sequence of PTMS strengthening in joints: (a) 2nd floor, (b) 1st floor, and (c) gap between steel plates and concrete faces to secure the 2 layer metal straps
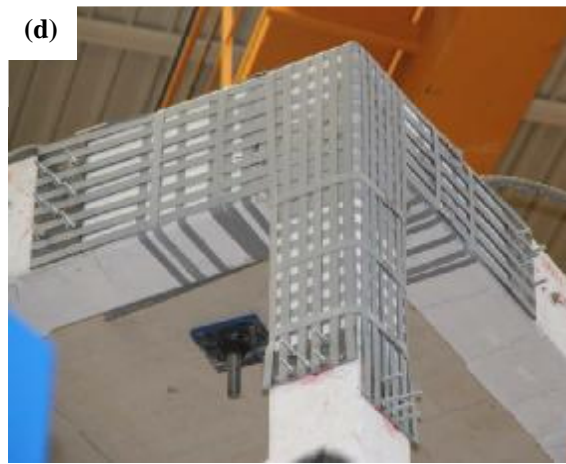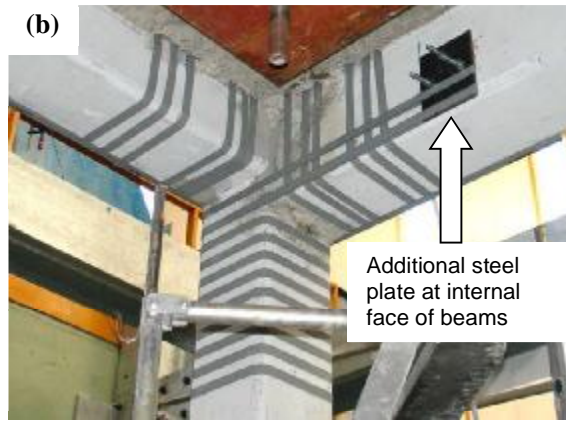
Fig. 11. PTMS strengthening of beam-column joints: (a) fixing of steel plates, (b) additional anchorage plate at interior face of beams, (c) final view of 1st floor joints, (d) final view of 2nd floor joints.
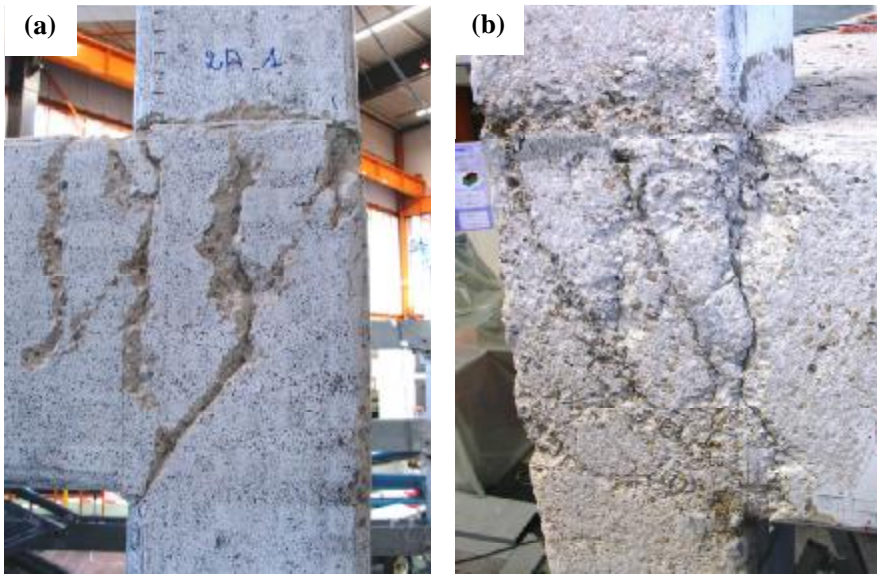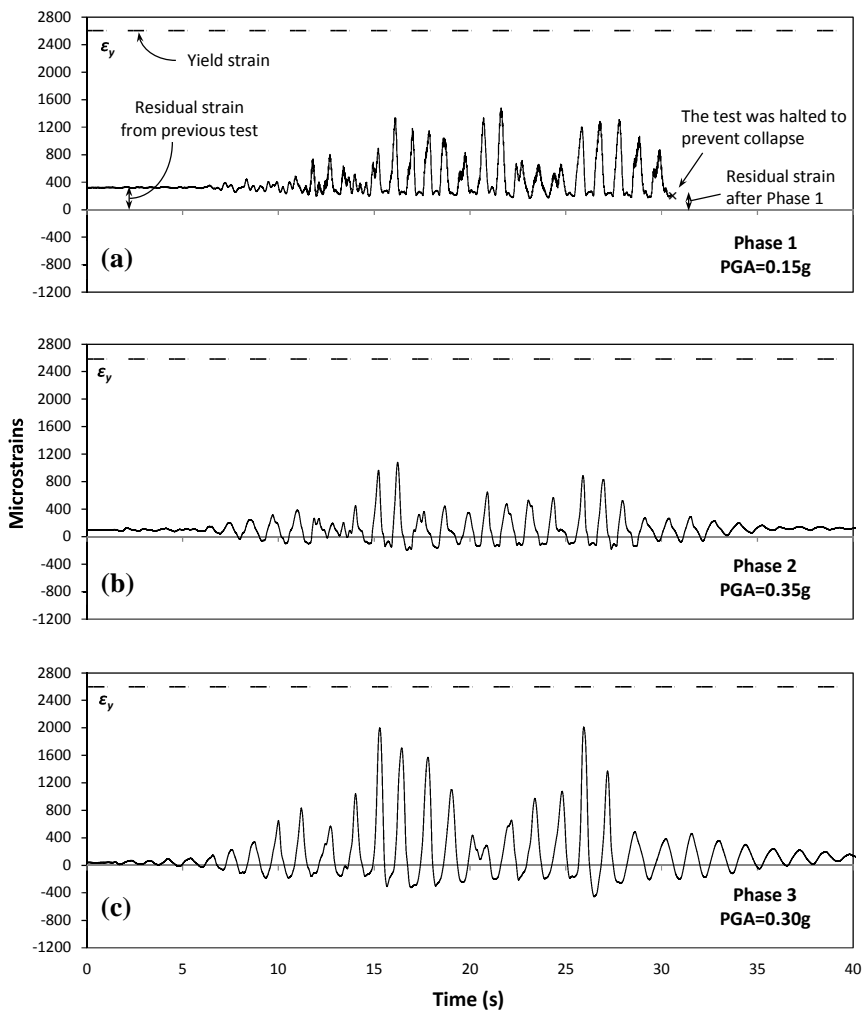
Fig. 12. Damage in beam-column joints after removal of PTMS in Phase 3: (a) J2A-1X, and (b) J1A-1X
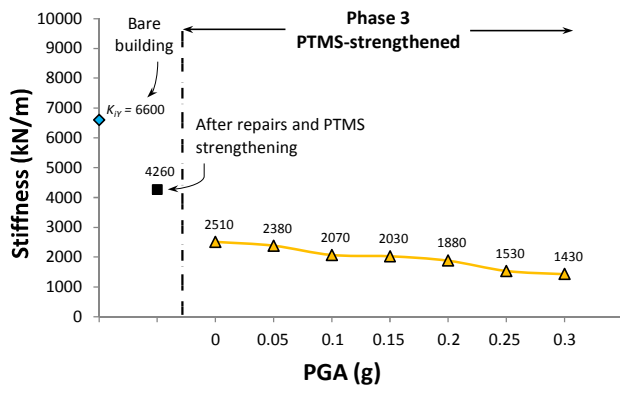
Fig. 13. Lateral stiffness degradation, Phase 3 (Y direction)
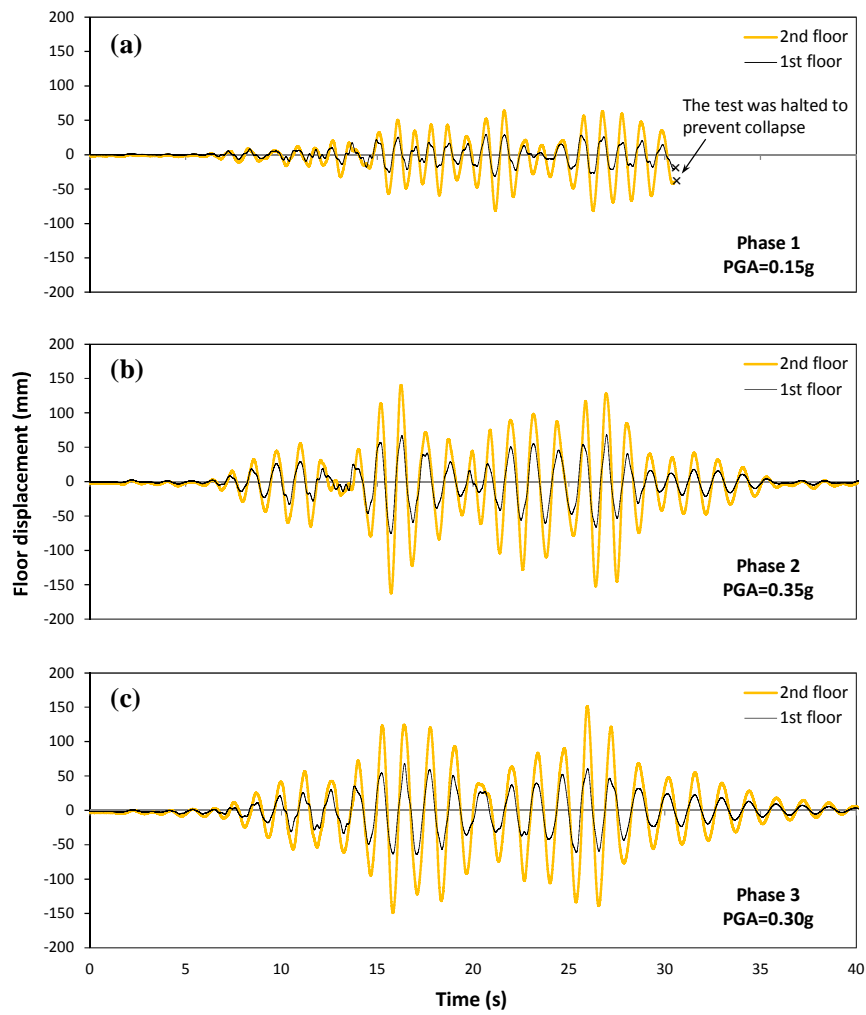
Fig. 14. Displacement time-histories of 1st and 2nd floors, last test of Phases 1 to 3

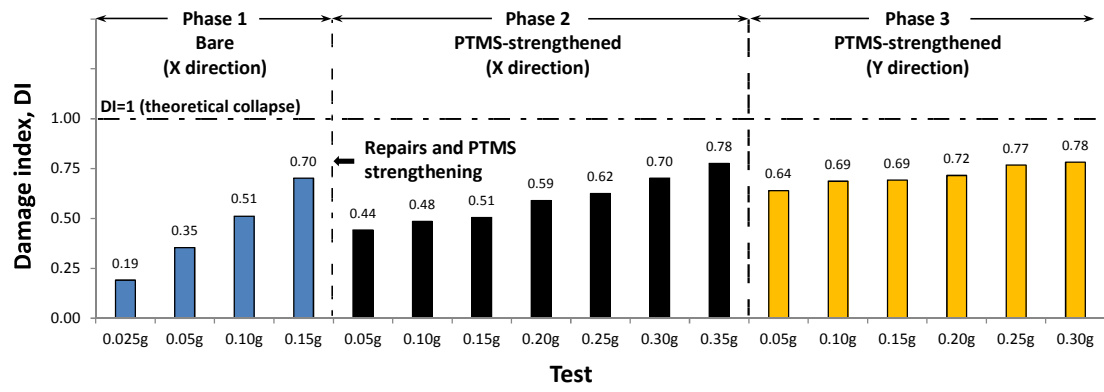**Fig. 15.** Strain time-histories of bottom beam reinforcement at joints, last test of Phases 1 to 3

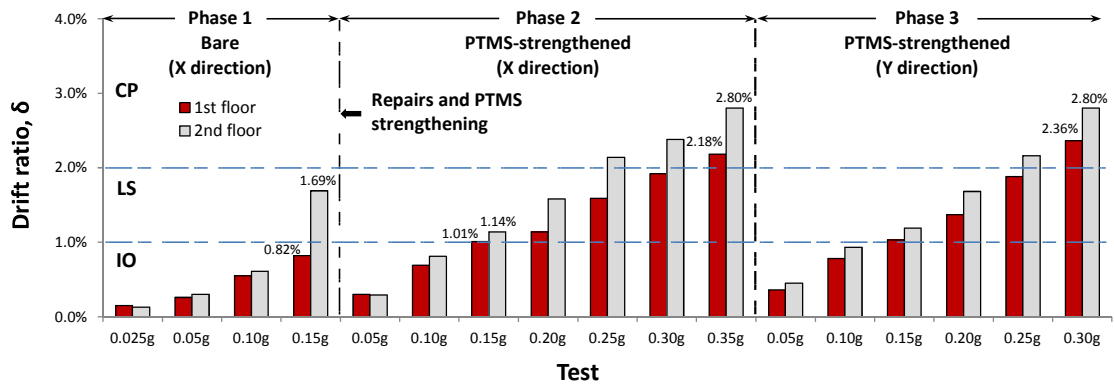**Fig. 16.** Global damage indices, Phases 1 to 3

Fig. 17. Inter-storey drift ratio of 1st and 2nd floors, Phases 1 to 3